

1 **Title:**

2 Tracing a protein's folding pathway over evolutionary time using ancestral sequence
3 reconstruction and hydrogen exchange

4

5 **Authors:**

6 Shion A. Lim^{1,2,5}, Eric R. Bolin^{2,3,5}, Susan Marqusee^{1,2,4}

7

8 ¹ Department of Molecular and Cell Biology, University of California, Berkeley, Berkeley,
9 CA, United States

10 ² Institute for Quantitative Biosciences (QB3), University of California, Berkeley,
11 Berkeley, CA, United States

12 ³ Biophysics Graduate Program, University of California, Berkeley, Berkeley, CA, United
13 States

14 ⁴ Department of Chemistry, University of California, Berkeley, Berkeley, CA, United
15 States

16 ⁵ The authors contributed equally to this work

17

18 Corresponding Author: Susan Marqusee, marqusee@berkeley.edu

19

20 **Keywords:** protein folding, hydrogen exchange, protein evolution, ancestral sequence
21 reconstruction, mass spectrometry

22

23

1 **Abstract:**

2 The conformations populated during protein folding have been studied for
3 decades; yet, their evolutionary importance remains largely unexplored. Ancestral
4 sequence reconstruction allows access to proteins across evolutionary time, and new
5 methods such as pulsed-labeling hydrogen exchange coupled with mass spectrometry
6 allow determination of folding intermediate structures at near amino-acid resolution.
7 Here, we combine these techniques to monitor the folding of the ribonuclease H family
8 along the evolutionary lineages of *T. thermophilus* and *E. coli* RNase H. All homologs
9 and ancestral proteins studied populate a similar folding intermediate despite being
10 separated by billions of years of evolution. Even though this conformation is conserved,
11 the pathway leading to it has diverged over evolutionary time, and rational mutations
12 can alter this trajectory. Our results demonstrate that evolutionary processes can affect
13 the energy landscape to preserve or alter specific features of a protein's folding
14 pathway.

15

1 **Introduction:**

2 Protein folding, the process by which an unfolded polypeptide chain navigates its
3 energy landscape to achieve its native structure,^{1,2} can be defined by the partially folded
4 conformations (intermediates) populated during this process. Such intermediates are
5 key features of the landscape; they can facilitate folding, but they can also lead to
6 misfolding and aggregation, resulting in a breakdown of proteostasis and disease.³⁻⁵
7 While identifying and characterizing these intermediates is critical to understanding and
8 engineering a protein's energy landscape, their transient nature and low populations
9 present experimental challenges. Recent technological improvements in hydrogen
10 exchange monitored by mass spectrometry (HX-MS) have provided access to the
11 structural and temporal details of these folding intermediates at near-single amino-acid
12 resolution.⁶⁻¹¹ This pulsed-labeling HX-MS approach is particularly well suited to studies
13 of multiple variants or families of proteins, as it does not require large amounts of
14 purified protein or NMR assignments. Thus, pulsed-labeling HX-MS can be used to
15 address long-standing questions in the field: How robust is a protein's energy landscape
16 to changes in the amino acid sequence, and how conserved is the folding trajectory
17 over evolutionary time?

18 Ribonuclease HI (RNase H) is an ideal system to investigate protein folding over
19 evolutionary time. RNase H from *E. coli*, ecRNH* (the asterisk denotes a cysteine-free
20 variant of RNase H), is arguably one of the best-characterized proteins in terms of its
21 folding pathway and energy landscape. Both stopped-flow ensemble studies and single-
22 molecule optical trap experiments demonstrate that this protein populates a major
23 obligate intermediate before the rate-limiting step in folding.¹²⁻¹⁶ A rare population of this

1 intermediate can also be detected under native-state conditions.¹⁷ Several homologs of
2 RNase H have also been studied, yielding insight into the folding trends of extant
3 RNases H.^{18–20}

4 In addition to comparing the folding pathways of homologs, one can use a
5 phylogenetic technique called ancestral sequence reconstruction (ASR) to access the
6 evolutionary history of a protein family and study the properties of ancestral
7 proteins.^{21,22} ASR has been applied to a variety of protein families and in addition to
8 revealing the evolutionary history, these ancestral proteins can act as intermediates in
9 sequence space to uncover mechanisms underlying protein properties.^{23–30} Recently,
10 ancestral sequence reconstruction was applied to the RNase H family and the
11 thermodynamic and kinetic properties of seven ancestral proteins connecting the
12 lineages of *E. coli* and *T. thermophilus* RNase H (ecRNH* and ttRNH*) were
13 characterized.^{31–33} Stopped-flow kinetics monitored by circular dichroism (CD)
14 demonstrate that all seven ancestral proteins populate a folding intermediate before the
15 rate-limiting step. Additionally, the folding and unfolding rates show notable trends along
16 the phylogenetic lineages, and the presence of a folding intermediate plays an important
17 role in modulating these evolutionary trends.³²

18 For ecRNH*, multiple methods have confirmed the structural details of the folding
19 intermediates. This major folding intermediate, termed I_{core}, which forms before the rate
20 limiting step, involves secondary structure from the core region of the protein, including
21 Helices A-D and Strands 4 and 5, while the rest of the protein (Helix E and Strands 1, 2,
22 3), remains unfolded (Figure 1A).^{12,34,35} Pulsed-labeling HX-MS with near amino acid
23 resolution was developed using ecRNH* as the model protein.⁶ This approach

1 confirmed the structure of I_{core} and revealed the stepwise protection of individual helices
2 leading up to the intermediate. Specifically, the amide hydrogens in Helix A and Strand
3 4 are the first elements to gain protection, followed by those in Helix D and Strand 5,
4 and then Helices B and C to form the canonical I_{core} intermediate. The periphery,
5 comprising of Strands 1-3 and Helix E, gains protection in the rate-limiting step to the
6 native state. Would this I_{core} folding intermediate and the stepwise folding pathway be
7 conserved across evolution?

8 Here, we use pulsed-labeling HX-MS on the resurrected family of RNases H to
9 investigate the evolutionary and sequence determinants governing the folding trajectory.
10 Specifically, we find that the structure of the major folding intermediate (I_{core}) has been
11 conserved over three billion years of evolution, suggesting that this partially folded state
12 plays a crucial role in the folding or function of the protein. The detailed steps leading to
13 this folding intermediate, however, vary. The very first step in folding differs between the
14 two extant homologs: for ecRNH*, Helix A gains protection before Helix D, while for
15 ttRNH*, Helix D acquires protection before Helix A. This pattern can be followed along
16 the evolutionary lineages: most of the ancestors fold like ttRNH* (Helix D before Helix A)
17 and a switch to fold like ecRNH* (Helix A before Helix D) occurs late along the
18 mesophilic lineage. These phylogenetic trends allow us to investigate how these early
19 folding events are encoded in the amino acid sequence. By selectively modulating
20 biophysical properties, notably intrinsic helicity, of specific secondary structure
21 elements, we are able to favor or disfavor the formation of specific conformations during
22 folding and have engineering control over the folding pathway of RNase H.

1 **Results:**

2 **Monitoring a protein's folding trajectory by pulsed-labeling HX-MS**

3 We used pulsed-labeling hydrogen exchange monitored by mass spectrometry
4 (HX-MS) on extant, ancestral, and site-directed variants of RNase H to examine the
5 robustness of a protein's folding pathway to sequence changes. These experiments
6 allow us to characterize the partially folded intermediates and the order of structure
7 formation during folding to ask whether these intermediates have changed over
8 evolutionary time, and what role sequence might play in determining these
9 intermediates.

10 Figure 1B outlines the scheme for the pulsed-labeling experiment (for details, see
11 Methods). Briefly, folding is initiated by rapidly diluting an unfolded (high [urea]), fully
12 deuterated protein into folding conditions (low [urea]) at 10°C. After various folding times
13 (t_f), a pulse of hydrogen exchange is applied to label amides in regions that have not yet
14 folded. The amount of exchange at each folding timepoint is then detected by in-line
15 proteolysis and LC/MS. Data are analyzed first at the peptide level by monitoring the
16 protection of deuterons on peptides as a function of refolding time, and then at the
17 residue level, using overlapping peptides de-convoluted by the program HDsite.^{36,37}

18 Since the original folding studies on RNase H were carried out at 25°C, we re-
19 characterized the folding of each RNase H variant at 10°C using stopped-flow circular
20 dichroism spectroscopy (Figure S1). The refolding profiles were consistent with those at
21 25°C.^{12,19,32} At low [urea], all ancestors show a large signal change (burst phase) within
22 the dead time of the stopped-flow instrument (~15 msec), followed by a slower
23 observable phase which fit well to a single exponential. The resulting chevron plots

1 ($\ln(k_{\text{obs}})$ vs [urea]) show the classic rollover at low [urea] due to the presence of a stable
2 folding intermediate. As expected, the observed rates at 10°C are slower than 25°C, but
3 the chevron profiles are similar for all RNase H variants. Thus the overall folding
4 trajectory, notably the population of a folding intermediate, has not changed between
5 the two temperatures.

6

7 **Monitoring the folding pathway of ttRNH* using pulsed-labeling HX-MS**

8 First, we characterized the conformations populated during folding of extant
9 RNase H from *T. thermophilus* and compared its folding trajectory to the previously
10 characterized folding trajectory of *E. coli* RNase H.⁶ 374 unique peptides were identified
11 by MS. Of these, 49 unique peptides were observed at all refolding time points and
12 were used for further analysis (Figure 2A). Similar to ecRNH*, peptides associated with
13 I_{core} (Helix A-D, Strands 4-5) gain protection early (within milliseconds), corresponding to
14 the timescale for the formation of the folding intermediate. Peptides associated with the
15 periphery of the protein (Strands 2-3, Helix E) gain protection on the order of seconds,
16 corresponding to the rate-limiting step (Figure 2B). Thus, the major folding intermediate
17 in ttRNH*, I_{core} , is strikingly similar to that of ecRNH*.⁶

18 Looking at the very early refolding times allows one to determine the individual
19 folding steps preceding I_{core} . At the earliest time point (~1 msec), almost all peptides
20 are unfolded (fully exchange with solvent) with the exception of those in Helix D and
21 Strand 5, which are ~40% deuterated (Figure 2C). Peptides spanning Helix A and
22 Strand 4 are less protected (~15% deuterated) at this same time point. This order of
23 protection (Helix D before Helix A) is notably different than that for *E. coli* RNase H*,

1 where Helix A is protected before Helix D.⁶ Peptides spanning Helix B and Helix C gain
2 protection in the I_{core} intermediate. Peptides from Strands 1-3 and Helix E do not gain
3 full protection until significantly later (on the order of seconds), corresponding to the
4 rate-limiting step to the native state. Thus, while the I_{core} intermediate is largely
5 conserved between ttRNH* and ecRNH*, the initial steps of folding differ between the
6 two homologs.

7 The peptide data from each time point were also analyzed using HDsite to
8 determine residue-level protection in a near site-resolved manner (Figure 2D). These
9 site-resolved data also show protection appearing first in Helix D and Strand 5, followed
10 by Helix A/Strand 4, Helix B/C, and finally, the periphery Helix E and Strands 1-3. The
11 differences in the order of protection leading up to I_{core} of ecRNH* and ttRNH* are also
12 evident in this site-resolved analysis.

13

14 **Pulsed-labeling HX-MS on the ancestral RNases H**

15 To look for evolutionary trends in the folding trajectory, we probed the folding
16 pathway of ancestral RNases H along the lineages of *E. coli* and *T. thermophilus* RNase
17 H (Figure 3A). Anc1* is the last common ancestor of ecRNH* and ttRNH*. Anc2* and
18 Anc3* are ancestors along the thermophilic lineage leading to ttRNH*, and AncA*,
19 AncB*, AncC*, and AncD* are ancestors along the mesophilic lineage leading to
20 ecRNH*. Previous kinetic studies demonstrated that all of the ancestral proteins fold via
21 a three-state pathway, populating an intermediate before the rate-limiting step.^{32,33} We
22 now use pulsed-labeling HX-MS to obtain a near-site resolved trajectory of the folding

1 pathway for each ancestor and determine whether the I_{core} structure is conserved over
2 evolution.

3 We obtained good peptide coverage for all of the ancestors with a minimum of 81
4 peptides seen in all time points for each variant (Figure 3, Figures S2-S7). As observed
5 in both ttRNH* (above) and ecRNH*⁶ all of the ancestral RNases H populate the
6 canonical I_{core} folding intermediate prior to the rate-limiting step. Peptides corresponding
7 to the I_{core} region of the RNase H structure become protected on the timescale of
8 milliseconds, while the rest of the protein gains protection on the timescale of seconds
9 (Figure 3C, Figures S2-S7). Thus, the structure of this major folding intermediate is not
10 only present in both extant RNases H, but is conserved over nearly three billion years of
11 evolutionary history.

12 Similarly to the extant proteins, the periphery of the ancestral proteins gains
13 protection on a much slower timescale (Figure 3C, Figure S2-S7). The details of
14 protection in this region, however, vary somewhat across the ancestors. The periphery
15 becomes fully protected by the last time point in all ancestral proteins except for AncB*
16 (Figure S5). AncB* was previously characterized to be non-two-state with a notable
17 population of the folding intermediate under equilibrium conditions,³² and the lack of
18 protection in the periphery in the folded state of AncB* is consistent with this
19 observation. For Anc1* and Anc2*, there are also notable differences in the time course
20 of protection for the terminal helix, Helix E. For these two proteins, the peptides
21 spanning Helix E are decoupled from Strands 1-3 (which show protection on the same
22 timescale as global folding) and do not gain protection even in the folded state of the
23 protein (Figure 3B, Figure 3D, Figure S2), suggesting that Helix E is improperly docked

1 or poorly structured in Anc1* and Anc2*. Indeed, Helix E is known to be labile in
2 ecRNH*: a deletion variant of ecRNH* without this final helix forms a cooperatively
3 folded protein,³⁸ and recent single-molecule force spectroscopy of ecRNH* showed that
4 Helix E can be pulled off the folded protein under low force while the remainder of the
5 protein remains structured (manuscript in preparation). It appears that Helix E may be
6 further destabilized in Anc1* and Anc2* such that it does not show protection in the
7 native state.

8

9 **The early folding steps of RNase H change across evolutionary time**

10 Since the order of events leading to I_{core} differs between the extant homologs, we
11 examined whether the ancestral RNases H spanning the lineages of these two
12 homologs show any trends in their early folding steps. For each ancestor, we analyzed
13 the fraction of deuterium protected in peptides that are uniquely associated with specific
14 helices of the protein (Figure 3D and Figure S2-S7) to determine which regions fold first.

15 These data show that the last common ancestor of ecRNH* and ttRNH*, Anc1*,
16 as well as all proteins along the thermophilic lineage (Anc2* and Anc3*) show similar
17 behavior to ttRNH* and gain protection first in Helix D/Strand 5 (Figure S2, S3). For the
18 first two ancestors along the mesophilic lineage (AncA* and AncB*), the order of
19 protection is difficult to determine. For AncA*, there is no significant difference in the
20 degree of protection among the peptides within I_{core} (this analysis is limited by the
21 availability of peptides associated exclusively within a region) (Figure S4). However,
22 when all overlapping peptides are analyzed using HDsite to obtain site resolution, we
23 observe notable protection in Helix D at the earliest refolding times. Therefore, we

1 conclude that although Helix D folding before Helix A is likely, the early folding events of
2 AncA* cannot be unambiguously determined. For AncB*, all of I_{core} gains protection at
3 the same time point, both at the peptide and residue-level, so the order of assembly
4 cannot be determined with our time resolution (Figure S5).

5 The next ancestor along the mesophilic lineage, AncC*, shows protection first in
6 Helix D, indicating that this pattern of protection is maintained through the mesophilic
7 lineage to this ancestor (Figure S6). AncD*, the most recent ancestor along the
8 mesophilic lineage, however, is similar to ecRNH* and gains protection first in Helix A
9 (Figure S7). As detailed for the other ancestors, the data were also analyzed using
10 HDSite to determine residue-level protection for each ancestral RNase H (Figure 3E,
11 Figure S2-S7). These data indicate a pattern in the order of protection in the early steps
12 of the folding pathway across the RNase H ancestors. Early protection in Helix D is an
13 ancestral feature of RNase H that is maintained in the thermophilic lineage, with a
14 transition occurring late during the mesophilic lineage to a different pathway where Helix
15 A is protected before Helix D, resulting in a distinct folding pathway for the two extant
16 RNase H homologs (Figure 4).

17

18 **Early helix protection is determined by the local sequence of the core**

19 Relative to the vast sequence space available, these RNase H ancestors
20 represent a set of closely related sequences with distinct folding properties and provide
21 an excellent system to help us elucidate the physiochemical mechanism and the
22 sequence determinants dictating the RNase H folding trajectory. An analysis of the
23 intrinsic helical propensity of each region using the algorithm AGADIR³⁹ shows a

1 notable trend in helicity that correlates with the early folding events (Figure 4). For
2 proteins that gain protection in Helix A first, the intrinsic helicity of Helix A is four-fold
3 higher than that of Helix D. For the variants where Helix D is protected first, the intrinsic
4 helicity of Helix D is similar to or greater than Helix A. This suggests that intrinsic helix
5 propensity may play an important role in determining which region is the first to gain
6 protection during the folding pathway of RNase H. To investigate this hypothesis, we
7 turned to rationally designed variants.

8

9 **Intrinsic helicity plays a role in determining the structure of the early** 10 **intermediates**

11 If the order of protection in the early folding events of RNase H is determined by
12 intrinsic helix propensity, then we should be able to alter the protein sequence rationally
13 and manipulate the folding trajectory. Thus, we asked whether single-site mutations that
14 change the relative helix propensity of Helix A and Helix D could alter the folding
15 trajectory of ecRNH* and make it fold in a similar fashion to ttRNH*. Two different point
16 mutations were made in ecRNH*: A55G decreases helix propensity in Helix A, and
17 D108L increases helicity in Helix D (Figure 4, Figure 5A, Table S1). Pulsed-labeling HX-
18 MS indicates that both of these variants alter the early folding events of ecRNH*. The
19 peptide-level protection of ecRNH* A55G indicates that at 13 msec, both Helix A and
20 Helix D show similar levels of protection. In contrast, for wild-type ecRNH*, Helix A
21 shows protection by 1 msec and Helix D does not show comparable protection until 10-
22 20 msec.⁶ Thus, the mutation A55G slows the gain of protection in Helix A such that it
23 no longer protected before Helix D (Figure 5B). The peptide-level protection of ecRNH*

1 D108L indicates a change in the order of protection. Due to the limited number of
2 peptides available, we could only confidently determine this using peptides spanning the
3 N-terminus of Helix D. At 13 msec, the N-terminus of Helix D (residues 106-108) near
4 the D108L mutation is protected significantly faster than any other region of the protein.
5 Thus increasing helix propensity correlated with a change in the folding trajectory.
6 (Figure 5C). Together, these two mutations suggest that intrinsic helicity plays a role in
7 the early folding events of RNase H and can be used to alter the stepwise order of
8 conformations populated during folding.

9

10

11 **Discussion:**

12 **Determining the folding pathway of multiple protein variants**

13 Pulsed-labeling hydrogen exchange is currently the most detailed method to
14 identify the conformations populated during protein folding. This approach was initially
15 developed for use with NMR detection where it benefited from NMR's site-specific
16 resolution of individual amides.⁴⁰ However, using NMR with pulsed-labeling HX requires
17 tens of milligrams of sample and NMR peak assignments for the amides in each protein
18 studied. In addition, probes are limited to amide sites stable to exchange in the final
19 folded state (protection factors of $>\sim 80,000$) resulting in loss of information at individual
20 sites, which can sometimes represent large regions of the protein. In contrast, detection
21 by mass spectrometry as applied in this study requires much less protein sample, has
22 much faster data collection, and can theoretically cover 100% of the protein sequence.
23 Importantly, this approach does not demand any structural information of the folded

1 state, such as NMR assignments, for the specific protein or variant studied. These
2 advantages enabled us to obtain the stepwise folding pathway of nine variants of
3 RNase H and study the evolutionary history and sequence determinants of the RNase H
4 folding pathway in detail. While pulsed-labeling HX-MS has been used to characterize
5 the folding pathways of several model systems, this study is the first to utilize the higher
6 throughput nature of HX-MS to study an ensemble of protein variants. The advantages
7 of this technique to study many different sequences of the same fold shows great
8 promise for probing the relationship between amino acid sequence and a protein's
9 energy landscape and will likely be particularly valuable for protein engineering and
10 design applications.

11 12 **I_{core} is a structurally conserved folding intermediate over 3 billion years of** 13 **evolution**

14 The native fold of a protein is robust to changes in sequence, proteins with
15 >~30% sequence identity share the same fold.⁴¹ Thus small variations in sequence,
16 such as those found among homologs or site-specific mutations, do not affect the
17 overall three-dimensional structure of a protein. These mutations can, however, affect
18 the overall energy landscape, which in turn can have profound effects of function. Here,
19 we find conservation of a high-energy structure populated during the folding of the
20 RNase H family over incredibly long evolutionary timescales. Using pulsed-labeling HX-
21 MS we identified and characterized the structure of the major folding intermediate in
22 seven ancestral and several mutant RNases H, which together with previous studies on

1 extant homologs, suggest that the conservation of this intermediate is a key feature of
2 the RNase H energy landscape across ~3 billion years of evolutionary time.

3 Why does I_{core} persist on the energy landscape of RNase H? One explanation is
4 a simple topological constraint; all RNases H may need to fold via a populated I_{core}
5 intermediate to successfully reach the native state. This explanation, however, is
6 countered by a previous study where a single mutation (I53D) in ecRNH* destabilizes
7 I_{core} such that it is no longer populated during folding—yet this variant still folds to the
8 native state.³⁴ Adding osmolytes, such as sodium sulfate, stabilizes this folding
9 intermediate and switches ecRNH* I53D back to a three-state folding pathway, showing
10 that the presence of the folding intermediate can be modulated. Additionally, a fragment
11 of RNase H containing only the I_{core} sequence (and variants thereof) can autonomously
12 fold and be studied at equilibrium, indicating that this structure is stable and robust to
13 mutations.^{42,43} The nature of the rate-limiting step, or folding barrier, which allows for the
14 buildup of this intermediate is unclear. One possibility is that the I_{core} intermediate is
15 populated simply because the information for folding this region is completely encoded
16 locally and I_{core} can fold relatively fast, before this rate limiting step to the fully folded
17 state.

18 Alternatively, I_{core} could be conserved because it contributes to the biological
19 function or fitness of the protein. Partially folded states and high-energy non-native
20 conformations are known to be important for a variety of protein functions and
21 proteostasis.^{4,44,45} All of the ancestral RNases H we studied here are active, in that they
22 cleave RNA-DNA hybrids in vitro,³¹ and although the residues thought to contribute to
23 substrate-binding affinity are contained in the core region of the protein,⁴⁶ the active site

1 residues (D10, E48, D70) span both the core and the periphery. It is therefore possible
2 that a stable folding core with an energetically independent periphery is important for
3 the efficiency or dynamics associated with catalysis in RNase H.

4 While the presence of the I_{core} intermediate has been observed in all proteins
5 studied here, recent studies have suggested that some of the RNase H variants, notably
6 for proteins along the thermophilic lineage, the I_{core} folding intermediate may also
7 involve structure in the first β -strand.^{33,43,47} While we see slight protection in this region
8 for ttRNH*, hydrogen exchange may not be the best probe of this—docking of Strand 1
9 without its hydrogen-bonding partners in the rest of the β -sheet may not be reflected by
10 backbone amide protection. Therefore, amide protection may not be observed even if
11 Strand 1 docks early to the core. The involvement of Strand 1 in ancestral other RNase
12 H variants studied remains unclear from this study.^{33,43}

13

14 **Aspects of the folding pathway are malleable across evolutionary time**

15 Our pulsed-labeling HX-MS results also illustrate how other features of a
16 protein's energy landscape can be altered over evolutionary timescales. Although the
17 I_{core} intermediate is conserved across all RNases H studied, the individual folding steps
18 leading up to I_{core} differ. Anc1*, the last common ancestor, folds through a pathway
19 where the Helix D/Strand 5 region is the first structural element to gain protection. This
20 ancestral feature is maintained along the thermophilic lineage to the extant ttRNH*.
21 Along the mesophilic branch, we observe a switch from this ancient folding pathway to
22 one that first forms protection in Helix A/Strand 4 that occurs evolutionarily between
23 AncC* and AncD*. This suggests that while the structure of I_{core} has been conserved

1 across 3 billion years of evolution, the steps to form this intermediate are malleable over
2 time. Since an isolated helix is unlikely show protection by HX, we expect additional
3 hydrophobic collapse of the polypeptide to contribute to the observed protection.
4 Nonetheless, the switch in protection between Helix A and Helix D indicates that
5 formation of native structure nucleates in a different region of the protein across the
6 RNase H variants studied, with a clear evolutionary trend.

7 Despite these trends, it remains difficult to rationalize these observations in terms
8 of a selective evolutionary pressure or fitness implication. These very early events occur
9 on the order of one millisecond, significantly faster than the overall folding of the protein.
10 Furthermore, all of these RNase H proteins fold to their native state efficiently with no
11 evidence for aggregation or misfolding. So, although partially folded states have been
12 implicated as gateways for aggregation for some proteins,⁴ this does not appear to be
13 the case for RNase H. It is possible that the change in the early folding step is a result
14 of mutations that are coupled to another feature under selection or drift. Although the
15 actual evolutionary implication for the RNase H folding pathway may be lost in history,
16 the trend in folding pathway across evolutionary time demonstrates that folding
17 pathways and conformations on the energy landscape of proteins can be affected over
18 time, and this system provides an excellent tool to interrogate the role sequence plays
19 in guiding the process of protein folding.

20

21 **The folding pathway of RNase H can be altered using simple sequence changes**

22 Our study also shows how insights from evolutionary history can contribute to our
23 understanding of the physiochemical mechanisms dictating the protein energy

1 landscape and how we might use that knowledge to engineer the landscape. The
2 regions that gain protection first involve helical secondary structure elements, and their
3 folding order correlates with isolated helical propensity of these regions predicted by
4 AGADIR.³⁹ Proteins where protection is first observed in Helix A have higher intrinsic
5 helicity in Helix A than in Helix D. Proteins where Helix D gains protection first higher
6 helicity in Helix D or roughly equal helicity in both regions This property was used to
7 guide our site-directed mutagenesis to select variants to alter the folding trajectory of
8 ecRNH* in a predictive manner using intrinsic helicity as a guide..

9 While these results are consistent with local helicity as a determinant of the
10 earliest folding steps, there may be other parameters that dictate the formation of these
11 conformations. The parameter average area buried upon folding (AABUF)⁴⁸ which
12 measures the average change in surface area of a residue from an unfolded state to a
13 folded state, has been shown to correlate to the structure of the folding intermediate in
14 apomyoglobin.^{49,50} Both helicity and AABUF are altered in the mutants considered in our
15 study (Table S1). Indeed, AABUF and helicity are often correlated and contributions of
16 either parameter are difficult to disentangle. Nevertheless, our data suggest that
17 parameters that are locally encoded in regions of a protein can be used engineer the
18 energy landscape of a protein including its folding pathway.

19 We have used a combination of ASR and pulsed-labeling HX-MS to explore the
20 conformations populated during the folding of multiple RNase H proteins, including
21 homologs, ancestors, and single-site variants. All RNase H proteins studied populate
22 the same major folding intermediate, I_{core}, indicating that this conformation has been
23 maintained on the energy landscape of RNase H over long evolutionary timescales (>3

1 billion years). This remarkable conservation of a partially folded structure on the energy
2 landscape of RNase H is contrasted with changes in the folding pathway leading up to
3 this structure. The early folding events preceding this intermediate (Helix A protected
4 before Helix D or vice versa) differ between the two homologs and also shows a notable
5 trend along the evolutionary lineages. This pattern of protection correlates with the
6 relative helix propensity of the sequences comprising these two helices, and we use this
7 knowledge to alter the folding pathway of ecRNH* through rationally designed
8 mutations. Our study illustrates how the energy landscape of a protein can be altered in
9 complex ways over evolutionary time scales, and how insights from evolutionary history
10 can contribute to our understanding of the physiochemical mechanisms dictating the
11 protein energy landscape.

12

13 **Acknowledgements:**

14 We thank members of the Marqusee Lab for helpful discussions. We also thank Leland
15 Mayne and members of the Englander Lab and Goran Stjepanovic in the Hurley Lab for
16 support on the pulsed-labeling HX-MS instrumental setup and analysis. We thank the
17 Vincent J. Coates Proteomics/Mass Spectrometry Facility for instrumentation support.
18 This work was funded by NIH Grant GM050945 (to S.M.) and a National Science
19 Foundation Graduate Research Fellowship (to S.A.L).

20

21 **Competing Interests:**

22 Authors declare no competing interests.

23

1

2 **Materials and Methods:**

3 **Protein Purification**

4 Cysteine-free *T. thermophilus* RNase H, and ancestral RNases H were expressed and
5 purified as previously described.^{31,51,52} Point mutants were generated using site-directed
6 mutagenesis, confirmed by Sanger sequencing, and the proteins were purified as
7 previously described.⁵³ Purity was confirmed by SDS-PAGE and mass spectrometry.

8

9 **HX-MS System**

10 Hydrogen exchange mass spectrometry (HX-MS) experiments were carried out using a
11 system similar to that described by Mayne et al.^{7,8} Briefly, a Bio-Logic SFM-4/Q quench
12 flow mixer with a modified head piece with reduced swept volume was used to initiate
13 protein refolding, followed by pulse-labeling unprotected amide hydrogen atoms, and
14 quenching of the labeling reaction. The minimum dead time for mixing is 13 msec.
15 Quenched samples were injected into an HPLC system constructed using two Agilent
16 1100 HPLC instruments. The quenched sample was flowed over columns (Upchurch
17 C130B) packed with beads of immobilized pepsin and fungal protease at 400 $\mu\text{L}/\text{min}$ in
18 0.05% TFA. The digested protein was run onto a C-4 trap column (Upchurch C-128 with
19 POROS R2 beads) for desalting. An acetonitrile gradient (15-100% acetonitrile, 0.05%
20 TFA at 17 $\mu\text{L}/\text{min}$) eluted peptides from this C-4 trap column and onto an analytical C-8
21 column (Thermo 72205-050565) for separation before injection into an ESI source for
22 mass spectrometry analysis on a Thermo Scientific LTQ Orbitrap Discovery. The entire
23 HPLC system is kept submerged in an ice bath at 0°C to reduce back exchange of

1 deuterium atoms during the chromatography steps. The workflow takes ~10-18 minutes
2 from injection to peptide detection.

3

4 **Refolding Experiment**

5 Similar to previous reports,^{6,8} unfolded protein samples in high denaturant (80 μ M
6 [protein], 20 mM NaOAc pH=4.1, 7-9 M [urea]) were deuterated by a repeated cycle of
7 lyophilization and resuspension in D₂O. For the pulsed labeling experiment, 1 volume of
8 deuterated protein was mixed in the SFM-4/Q with 10 volumes of refolding buffer (10
9 mM Sodium Acetate pH=5.29, H₂O) to initiate refolding. The pulse for hydrogen
10 exchange was initiated by mixing with 5 volumes of high pH buffer (100 mM Glycine
11 pH=10.11) and then quenched after 10 msec with 5 volumes low pH buffer (200 mM
12 Glycine pH=1.95). The length of the delay line between the first and second mixer was
13 changed to achieve a range of refolding times. An interrupted mixing protocol was used
14 to measure the longest refolding time points (>373 msec). Undeuterated protein was
15 used to perform tandem mass spectrometry (MS/MS) analysis to compile a list of
16 peptides and their retention times in the HPLC system. Competition experiments where
17 refolding and exchange were initiated at the same time were performed by diluting
18 deuterated protein in high urea into high-pH refolding buffer (100 mM Glycine
19 pH=10.11). In this experiment each site will exchange with the solvent around it unless it
20 can gain protection before exchange occurs (<1 msec on average). For each time point,
21 an identical sample was collected in which the high pH pulse was replaced by
22 unbuffered water to measure back exchange for each sample. All data were obtained in
23 triplicate and were normalized for back exchange. Data for ttRNH* were normalized to

1 the theoretical maximum number of deuterons as back exchange controls for this
2 protein did not produce enough peptides. Fully folded controls were created by diluting
3 unfolded protein samples 1:10 in fully deuterated refolding buffer and incubating at room
4 temperature for 4 hours before applying the same 10 msec high-pH pulse using the
5 SFM-4/Q.

6

7 **MS detection and data analysis**

8 Proteome Discoverer 2.0 (Thermo Scientific) was used to identify peptides from the
9 tandem MS data. Peptides identified in the pulse-labeled refolding experiments with
10 deuterated protein were used to determine the presence and deuteration level of each
11 peptide at each refolding time point. The spectral envelope of each peptide was fit using
12 two separate algorithms developed by the Englander Lab to determine their deuteration
13 state — ExMS for identification and fitting of peptides and HDsite for deconvolution of
14 overlapping peptides to achieve near-amino acid level deuteration levels.^{36,37} In
15 addition, HDExaminer (Sierra Analytics) was used to identify and fit each peptide and
16 determine deuteration levels. Different charge states of the same peptide were
17 averaged where noted and used for further analysis. Centroids of each peptide at each
18 time point taken from HDExaminer were used for further analysis. The residue cutoffs
19 for specific structural regions of each protein were determined from a multiple sequence
20 alignment using the structure of *E. coli* RNase H as a guide (PDB: 2RN2).³¹ Peptides
21 were assigned to different structural regions based on these residue cutoffs. Peptides
22 that spanned multiple secondary structural regions of a protein were excluded from
23 further analysis, as were peptides not present in all time points. Peptides mapping to

1 Strands 1-3 and Helix E were assigned to the periphery region of the protein. Peptides
2 mapping to Helix A-D and Strands 4-5 were assigned to the core region of the protein.

3

4 **References**

- 5 1. Dill, K. A. & MacCallum, J. L. The Protein-Folding Problem, 50 Years On. *Science*
6 **338**, 1042–1046 (2012).
- 7 2. Baldwin, R. L. Intermediates in Protein Folding Reactions and the Mechanism of
8 Protein Folding. *Annu. Rev. Biochem.* **44**, 453–475 (1975).
- 9 3. Karamanos, T. K. *et al.* A population shift between sparsely-populated folding
10 intermediates determines amyloidogenicity. *J. Am. Chem. Soc.* **138**, 6271–6280
11 (2016).
- 12 4. Chiti, F. & Dobson, C. M. Protein Misfolding, Amyloid Formation, and Human
13 Disease: A Summary of Progress Over the Last Decade. *Annu. Rev. Biochem.*
14 **86**, 27–68 (2017).
- 15 5. Ahn, M. *et al.* The Significance of the Location of Mutations for the Native-State
16 Dynamics of Human Lysozyme. *Biophys. J.* **111**, 2358–2367 (2016).
- 17 6. Hu, W. *et al.* Stepwise protein folding at near amino acid resolution by hydrogen
18 exchange and mass spectrometry. *Proc. Natl. Acad. Sci.* **110**, 7684–9 (2013).
- 19 7. Walters, B. T., Ricciuti, A., Mayne, L. & Englander, S. W. Minimizing Back
20 Exchange in the Hydrogen Exchange-Mass Spectrometry Experiment. *J. Am.*
21 *Soc. Mass Spectrom.* **23**, 2132–2139 (2012).
- 22 8. Mayne, L. *et al.* Many Overlapping Peptides for Protein Hydrogen Exchange
23 Experiments by the Fragment Separation-Mass Spectrometry Method. *J. Am.*

- 1 *Soc. Mass Spectrom.* **22**, 1898–1905 (2011).
- 2 9. Aghera, N. & Udgaonkar, J. B. Stepwise Assembly of β -Sheet Structure during
3 the Folding of an SH3 Domain Revealed by a Pulsed Hydrogen Exchange Mass
4 Spectrometry Study. *Biochemistry* **56**, 3754–3769 (2017).
- 5 10. Vahidi, S., Stocks, B. B., Liaghati-Mobarhan, Y. & Konermann, L. Submillisecond
6 Protein Folding Events Monitored by Rapid Mixing and Mass Spectrometry-Based
7 Oxidative Labeling. *Anal. Chem.* **85**, 8618–8625 (2013).
- 8 11. Khanal, A., Pan, Y., Brown, L. S. & Konermann, L. Pulsed hydrogen/deuterium
9 exchange mass spectrometry for time-resolved membrane protein folding studies.
10 *J. Mass Spectrom.* **47**, 1620–1626 (2012).
- 11 12. Raschke, T. M. & Marqusee, S. The kinetic folding intermediate of ribonuclease H
12 resembles the acid molten globule and partially unfolded molecules detected
13 under native conditions. *Nat. Struct. Biol.* **4**, 298–304 (1997).
- 14 13. Raschke, T. M., Kho, J. & Marqusee, S. Confirmation of the hierarchical folding of
15 RNase H: a protein engineering study. *Nat. Struct. Biol.* **6**, 825–831 (1999).
- 16 14. Cecconi, C., Shank, E. A., Bustamante, C. & Marqusee, S. Direct observation of
17 the three-state folding of a single protein molecule. *Science* **309**, 2057–2060
18 (2005).
- 19 15. Rosen, L. E., Connell, K. B. & Marqusee, S. Evidence for close side-chain
20 packing in an early protein folding intermediate previously assumed to be a
21 molten globule. *Proc. Natl. Acad. Sci.* **111**, 14746–14751 (2014).
- 22 16. Rosen, L. E., Kathuria, S. V., Matthews, C. R., Bilsel, O. & Marqusee, S. Non-
23 Native Structure Appears in Microseconds during the Folding of *E. coli* RNase H.

- 1 *J. Mol. Biol.* **427**, 443–453 (2015).
- 2 17. Chamberlain, A. K., Handel, T. M. & Marqusee, S. Detection of rare partially
3 folded molecules in equilibrium with the native conformation of RNase H. *Nat.*
4 *Struct. Biol.* **3**, 782–7 (1996).
- 5 18. Kern, G., Handel, T. M. & Marqusee, S. Characterization of a folding intermediate
6 from HIV-1 ribonuclease H. *Protein Sci.* **7**, 2164–2174 (1998).
- 7 19. Hollien, J. & Marqusee, S. Comparison of the folding processes of T.
8 thermophilus and E. coli ribonucleases H. *J. Mol. Biol.* **316**, 327–340 (2002).
- 9 20. Ratcliff, K., Corn, J. & Marqusee, S. Structure, stability, and folding of
10 ribonuclease H1 from the moderately thermophilic *Chlorobium tepidum*:
11 comparison with thermophilic and mesophilic homologues. *Biochemistry* **48**,
12 5890–5898 (2009).
- 13 21. Harms, M. J. & Thornton, J. W. Evolutionary biochemistry: revealing the historical
14 and physical causes of protein properties. *Nat. Rev. Genet.* **14**, 559–571 (2013).
- 15 22. Wheeler, L. C., Lim, S. A., Marqusee, S. & Harms, M. J. The thermostability and
16 specificity of ancient proteins. *Curr. Opin. Struct. Biol.* **38**, 37–43 (2016).
- 17 23. Starr, T. N., Picton, L. K. & Thornton, J. W. Alternative evolutionary histories in the
18 sequence space of an ancient protein. *Nature* **549**, 409–413 (2017).
- 19 24. Gaucher, E. A., Govindarajan, S. & Ganesh, O. K. Palaeotemperature trend for
20 Precambrian life inferred from resurrected proteins. *Nature* **451**, 704–707 (2008).
- 21 25. Hobbs, J. K. *et al.* On the origin and evolution of thermophily: reconstruction of
22 functional precambrian enzymes from ancestors of *Bacillus*. *Mol. Biol. Evol.* **29**,
23 825–835 (2012).

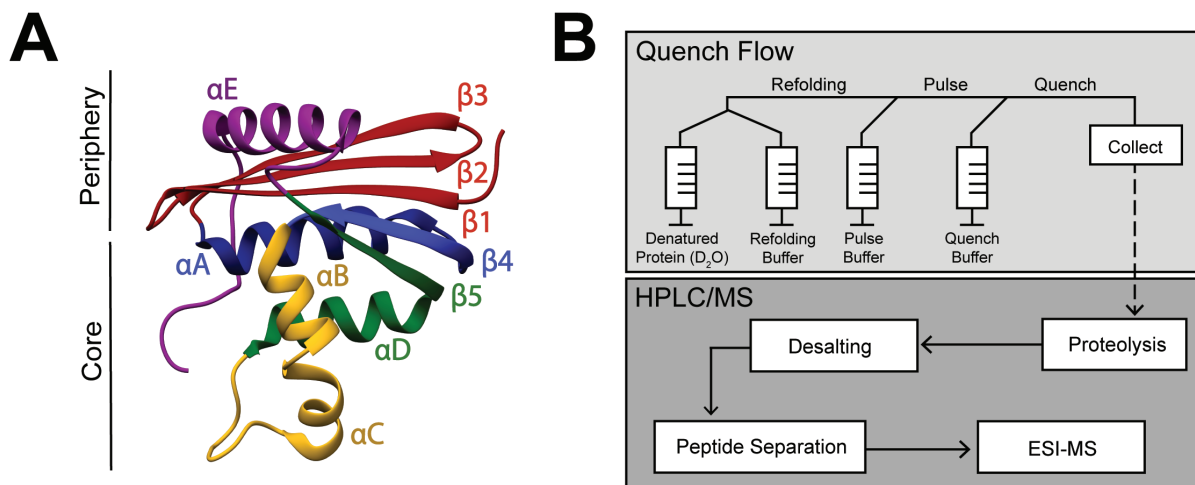
- 1 26. Perez-Jimenez, R. *et al.* Single-molecule paleoenzymology probes the chemistry
2 of resurrected enzymes. *Nat. Struct. Mol. Biol.* **18**, 592–596 (2011).
- 3 27. Risso, V. A., Gavira, J. A., Mejia-Carmona, D. F., Gaucher, E. A. & Sanchez-Ruiz,
4 J. M. Hyperstability and Substrate Promiscuity in Laboratory Resurrections of
5 Precambrian β -Lactamases. *J. Am. Chem. Soc.* **135**, 2899–2902 (2013).
- 6 28. Smock, R. G., Yadid, I., Dym, O., Clarke, J. & Tawfik, D. S. De Novo Evolutionary
7 Emergence of a Symmetrical Protein Is Shaped by Folding Constraints. *Cell* **164**,
8 476–486 (2016).
- 9 29. Akanuma, S. *et al.* Experimental evidence for the thermophilicity of ancestral life.
10 *Proc. Natl. Acad. Sci.* **110**, 11067–11072 (2013).
- 11 30. Siddiq, M. A., Hochberg, G. K. & Thornton, J. W. Evolution of protein specificity:
12 insights from ancestral protein reconstruction. *Curr. Opin. Struct. Biol.* **47**, 113–
13 122 (2017).
- 14 31. Hart, K. M. *et al.* Thermodynamic System Drift in Protein Evolution. *PLoS Biol.* **12**,
15 e1001994 (2014).
- 16 32. Lim, S. A., Hart, K. M., Harms, M. J. & Marqusee, S. Evolutionary trend toward
17 kinetic stability in the folding trajectory of RNases H. *Proc. Natl. Acad. Sci.* **113**,
18 13045–13050 (2016).
- 19 33. Lim, S. A. & Marqusee, S. The burst-phase folding intermediate of ribonuclease H
20 changes conformation over evolutionary history. *Biopolymers* e23086 (2017).
21 doi:10.1002/bip.23086
- 22 34. Spudich, G. M., Miller, E. J. & Marqusee, S. Destabilization of the Escherichia coli
23 RNase H Kinetic Intermediate: Switching Between a Two-state and Three-state

- 1 Folding Mechanism. *J. Mol. Biol.* **335**, 609–618 (2004).
- 2 35. Connell, K. B., Miller, E. J. & Marqusee, S. The folding trajectory of RNase H is
3 dominated by its topology and not local stability: a protein engineering study of
4 variants that fold via two-state and three-state mechanisms. *J. Mol. Biol.* **391**,
5 450–460 (2009).
- 6 36. Kan, Z.-Y., Walters, B. T., Mayne, L. & Englander, S. W. Protein hydrogen
7 exchange at residue resolution by proteolytic fragmentation mass spectrometry
8 analysis. *Proc. Natl. Acad. Sci.* **110**, 16438–16443 (2013).
- 9 37. Kan, Z.-Y., Mayne, L., Chetty, P. S. & Englander, S. W. ExMS: Data Analysis for
10 HX-MS Experiments. *J. Am. Soc. Mass Spectrom.* **22**, 1906–1915 (2011).
- 11 38. Goedken, E. R., Raschke, T. M. & Marqusee, S. Importance of the C-Terminal
12 Helix to the Stability and Enzymatic Activity of Escherichia coli Ribonuclease H.
13 *Biochemistry* **36**, 7256–7263 (1997).
- 14 39. Muñoz, V. & Serrano, L. Elucidating the folding problem of helical peptides using
15 empirical parameters. *Nat. Struct. Biol.* **1**, 399–409 (1994).
- 16 40. Bai, Y. Protein folding pathways studied by pulsed- and native-state hydrogen
17 exchange. *Chem. Rev.* **106**, 1757–1768 (2006).
- 18 41. Sander, C. & Schneider, R. Database of homology-derived protein structures and
19 the structural meaning of sequence alignment. *Proteins Struct. Funct. Genet.* **9**,
20 56–68 (1991).
- 21 42. Chamberlain, A. K., Fischer, K. F., Reardon, D., Handel, T. M. & Marqusee, S.
22 Folding of an isolated ribonuclease H core fragment. *Protein Sci.* **8**, 2251–2257
23 (1999).

- 1 43. Rosen, L. E. & Marqusee, S. Autonomously Folding Protein Fragments Reveal
2 Differences in the Energy Landscapes of Homologous RNases H. *PLoS One* **10**,
3 e0119640 (2015).
- 4 44. Baldwin, A. J. & Kay, L. E. NMR spectroscopy brings invisible protein states into
5 focus. *Nat. Chem. Biol.* **5**, 808–814 (2009).
- 6 45. Boehr, D. D., McElheny, D., Dyson, H. J. & Wright, P. E. The dynamic energy
7 landscape of dihydrofolate reductase catalysis. *Science* **313**, 1638–1642 (2006).
- 8 46. Kanaya, S., Katsuda-Nakai, C. & Ikehara, M. Importance of the positive charge
9 cluster in Escherichia coli ribonuclease HI for the effective binding of the
10 substrate. *J. Biol. Chem.* **266**, 11621–11627 (1991).
- 11 47. Zhou, Z., Feng, H., Ghirlando, R. & Bai, Y. The high-resolution NMR structure of
12 the early folding intermediate of the Thermus thermophilus ribonuclease H. *J. Mol.*
13 *Biol.* **384**, 531–539 (2008).
- 14 48. Rose, G. D., Geselowitz, A. R., Lesser, G. J., Lee, R. H. & Zehfus, M. H.
15 Hydrophobicity of amino acid residues in globular proteins. *Science* **229**, 834–838
16 (1985).
- 17 49. Nishimura, C., Lietzow, M. A., Dyson, H. J. & Wright, P. E. Sequence
18 Determinants of a Protein Folding Pathway. *J. Mol. Biol.* **351**, 383–392 (2005).
- 19 50. Nishimura, C., Dyson, H. J. & Wright, P. E. Consequences of Stabilizing the
20 Natively Disordered F Helix for the Folding Pathway of Apomyoglobin. *J. Mol.*
21 *Biol.* **411**, 248–263 (2011).
- 22 51. Robic, S., Berger, J. M. & Marqusee, S. Contributions of folding cores to the
23 thermostabilities of two ribonucleases H. *Protein Sci.* **11**, 381–389 (2002).

- 1 52. Hollien, J. & Marqusee, S. Structural distribution of stability in a thermophilic
2 enzyme. *Proc. Natl. Acad. Sci.* **96**, 13674–13678 (1999).
- 3 53. Dabora, J. M. & Marqusee, S. Equilibrium unfolding of Escherichia coli
4 ribonuclease H: characterization of a partially folded state. *Protein Sci.* **3**, 1401–
5 1408 (1994).
- 6 54. Ishikawa, K. *et al.* Crystal Structure of Ribonuclease H from Thermus
7 thermophilus HB8 Refined at 2·8 Å Resolution. *J. Mol. Biol.* **230**, 529–542 (1993).
- 8 55. Katayanagi, K. *et al.* Structural details of ribonuclease H from Escherichia coli as
9 refined to an atomic resolution. *J. Mol. Biol.* **223**, 1029–1052 (1992).
- 10
11

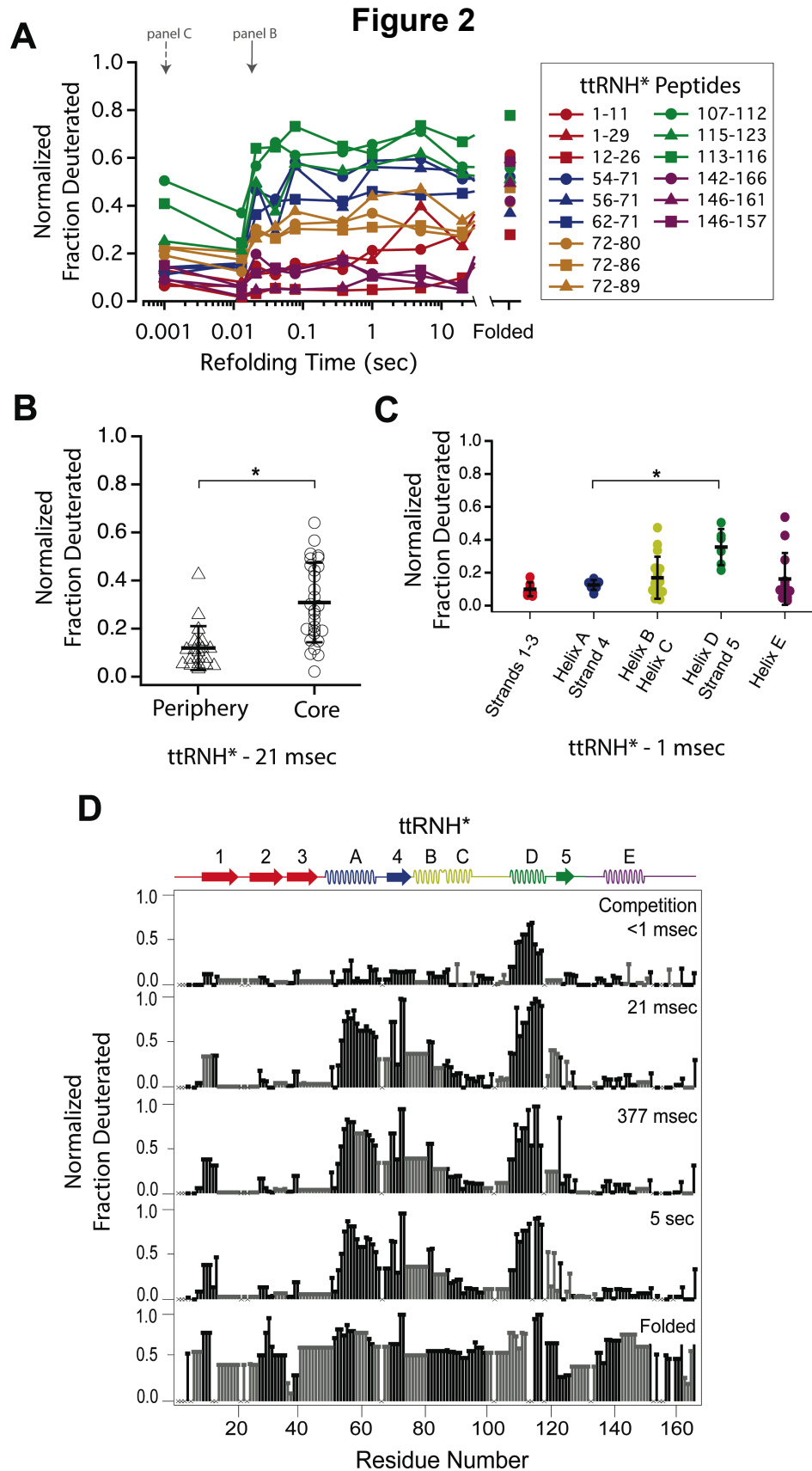
1 **Figures:**



2

3 **Figure 1. RNase H structure and Pulsed-labeling HX-MS**

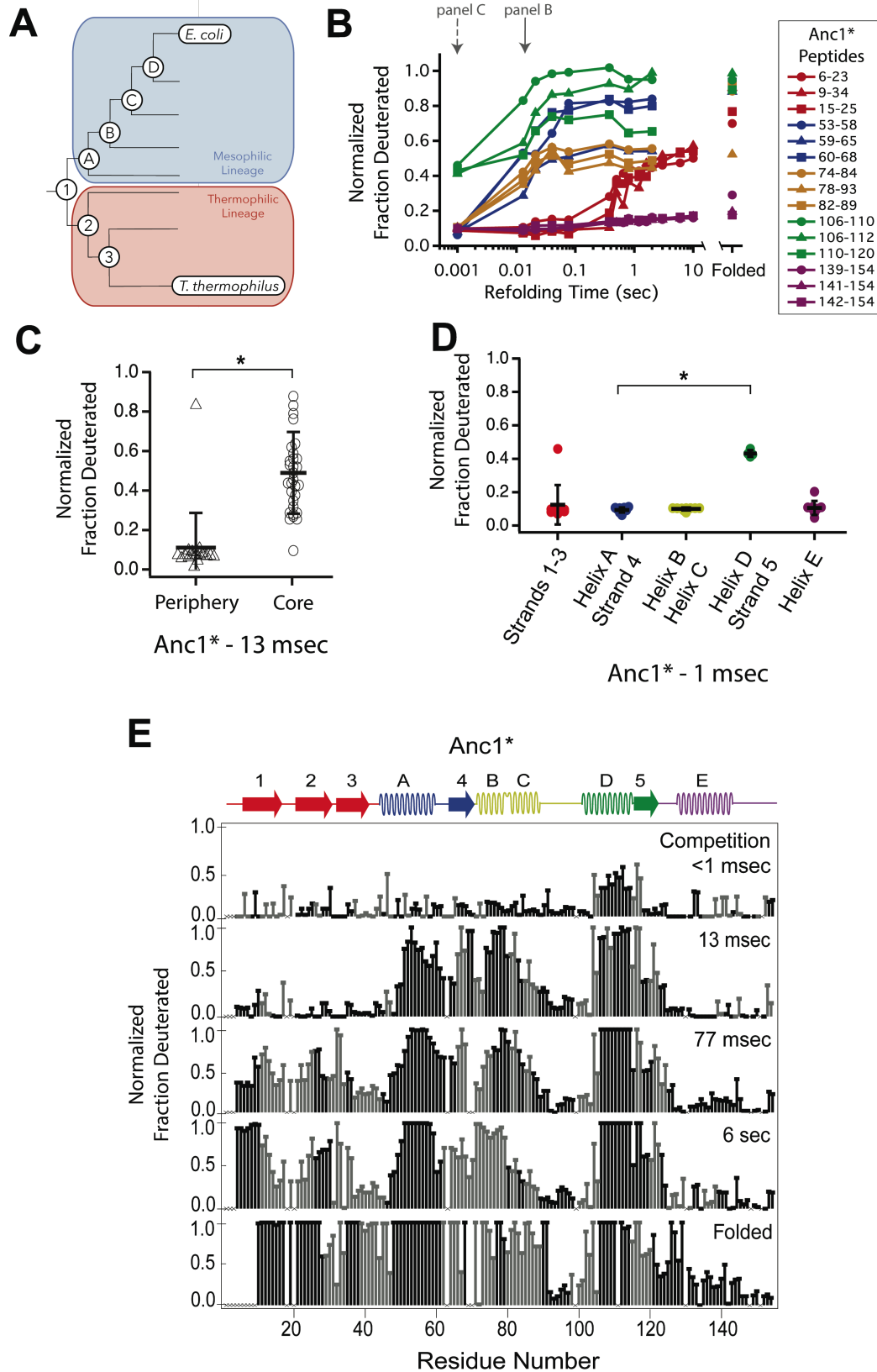
4 **A)** Crystal structure of *E. coli* RNase H* (ecRNH*) (PDB: 2RN2).⁵⁴ Secondary structural
5 elements: Red: Strand 1, Strand 2, Strand 3 (S123); Blue: Helix A, Strand 4 (HAS4);
6 Yellow: Helix B, Helix C (HBHC); Green: Helix D, Strand 5 (HDS5); Purple: Helix E
7 (HE). The core region of the protein (I_{core}) involving Helix A, Strand 4, Helix B, Helix C,
8 Helix D, Strand 5 and the periphery region of the protein involving Strand 1, Strand 2,
9 Strand 3, Helix E are denoted. **B)** Pulsed-labeling setup and workflow. Unfolded, fully
10 deuterated protein in high [urea] is rapidly mixed with low [urea] refolding buffer to
11 initiate refolding. After some refolding time, hydrogen exchange of unprotected amides
12 is initiated by mixing with high-pH pulse buffer. The hydrogen exchange reaction is
13 quenched by mixing with a low-pH quench buffer. The sample is injected onto an LC-
14 MS for in-line proteolysis, desalting, and peptide separation by reverse-phase
15 chromatography followed by MS analysis.



1 **Figure 2. Determination of the folding pathway of *T. thermophilus* RNase H* by**
2 **HX-MS**

3 **A)** Protection of representative peptides from ttRNH* at various refolding times.
4 Peptides are colored according to their corresponding structural element. The solid
5 arrow indicates the refolding time point analyzed in panel B. The dotted arrow indicates
6 the refolding time point analyzed in panel C. **B)** Protection of peptides mapping to the
7 core region (I_{core}) or the periphery region of ttRNH* at 21 msec after refolding. Bars
8 represent the mean and standard deviation of each data set. * $p < 0.0001$ (Welch's
9 unpaired T-test) **C)** Protection of peptides of ttRNH* mapping to distinct secondary
10 structural elements at 1 msec after refolding. Bars represent the mean and standard
11 deviation of each data set. * $p = 0.0027$ (Welch's unpaired T-test). **D)** Residue-resolved
12 folding pathway of ttRNH* at representative refolding time points. Data points in black
13 indicate residues that are site-resolved. Data points in grey indicate residues in regions
14 with less peptide coverage and are thus not site-resolved with the neighboring residues.
15 Residues where site-resolved protection could not be determined due to insufficient
16 peptide coverage is denoted with a "x".
17

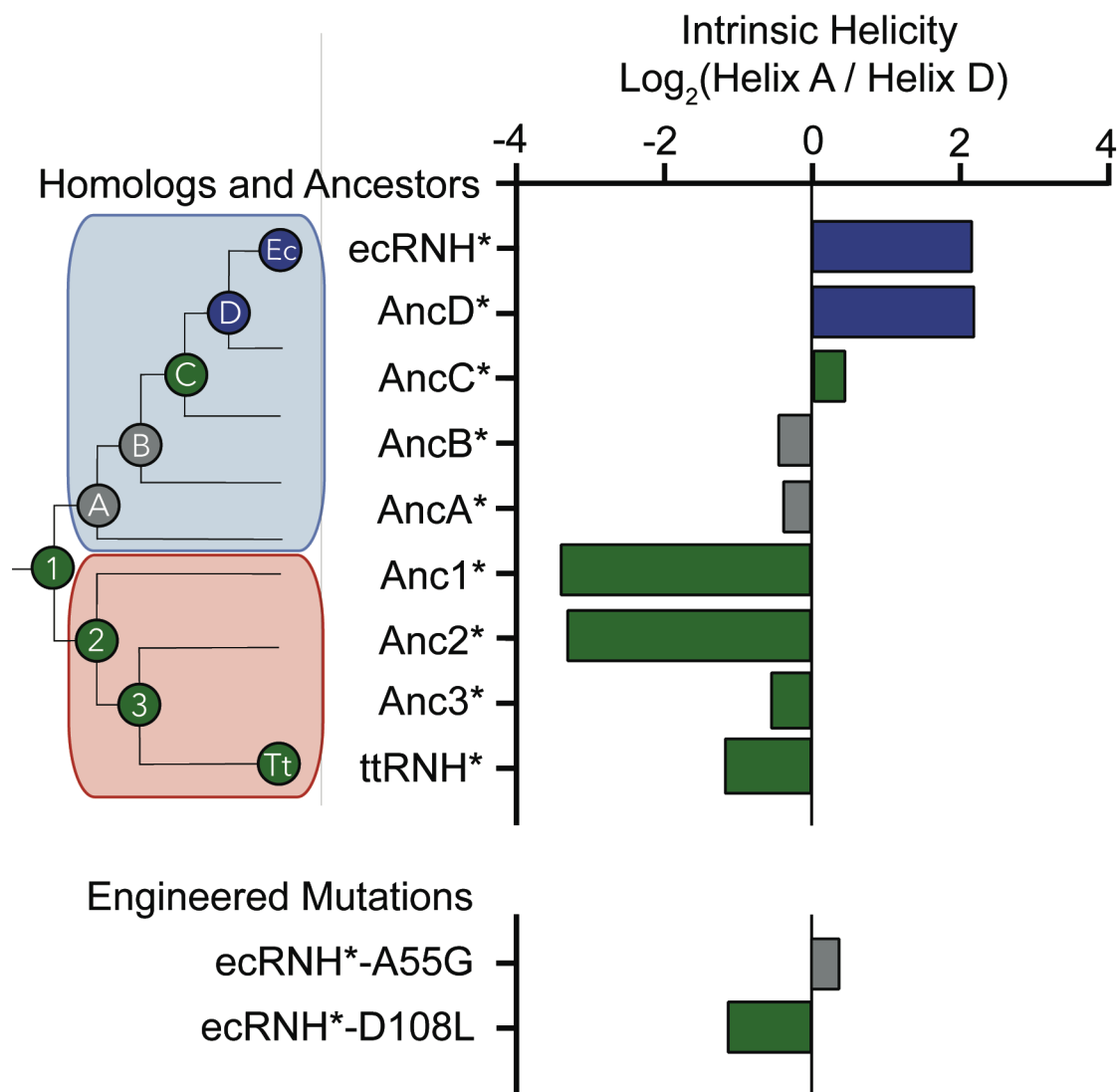
Figure 3



1 **Figure 3. Determination of the folding pathway of ancestral RNases H by HX-MS**

2 **A)** Representation of the phylogenetic tree of the RNase H family illustrating the
3 ancestral proteins along the two lineages leading to *E. coli* RNase H and *T.*
4 *thermophilus* RNase H. Adapted from Figure 2A of Hart KM et al. 2014, *PLoS Biology*.
5 12(11) doi:10.1371/journal.pbio.1001994, published under the Creative Commons
6 Attribution 4.0 International Public License (CC BY 4.0;
7 <https://creativecommons.org/licenses/by/4.0/>).³¹ Anc1* is the last common ancestor of
8 ecRNH* and ttRNH*. Anc2* and Anc3* are ancestors along the thermophilic lineage to
9 ttRNH*. AncA*, AncB*, AncC*, and AncD* are ancestors along the mesophilic lineage to
10 ecRNH*. **B)** Protection of representative peptides from Anc1* at various refolding times.
11 Peptides are colored according to their corresponding structural element. The solid
12 arrow indicates the refolding time point analyzed in panel B. The dotted arrow indicates
13 the refolding time point analyzed in panel C. **C)** Protection of peptides mapping to the
14 core region (I_{core}) or the periphery region of Anc1* at 13 msec after refolding. Bars
15 represent the mean and standard deviation of each data set. *p = 0.0011 (Welch's
16 unpaired T-test) **D)** Protection of peptides mapping to distinct secondary structural
17 elements of Anc1* at 1 milliseconds after refolding. Bars represent the mean and
18 standard deviation of each data set. *p < 0.0001 (Welch's unpaired T-test). **E)** Residue-
19 resolved folding pathway of Anc1* at representative refolding time points. Data points in
20 black indicate residues that are site-resolved. Data points in grey indicate residues in
21 regions with less peptide coverage and are thus not site-resolved with the neighboring
22 residues. Residues where site-resolved protection could not be determined due to
23 insufficient peptide coverage is denoted with a "x".

1



2

3

4 **Figure 4. Intrinsic helicity as a predictor for the early folding mechanism of**
5 **RNases H**

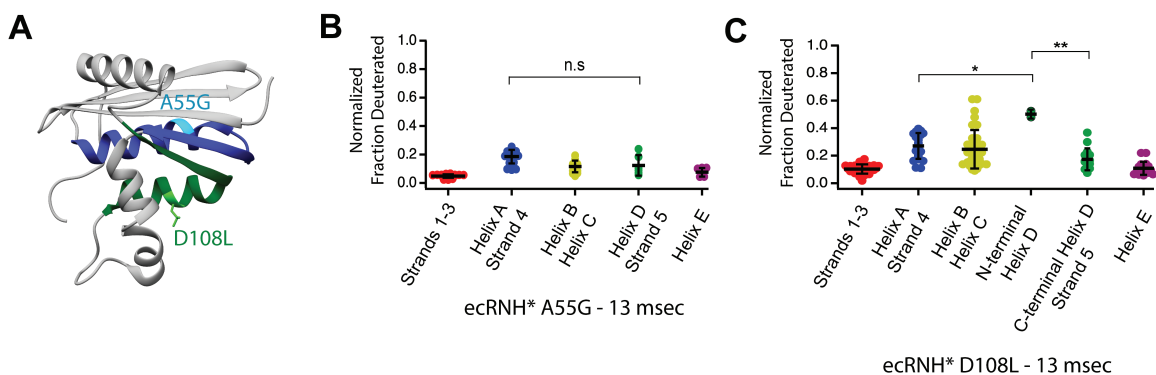
6 Log-ratio of intrinsic helicity of Helix A and Helix D for each RNase H variant studied.

7 Intrinsic helix predictions were calculated using AGADIR.³⁹ The order of helix protection

8 for each variant of RNase H is depicted in color. Green bars represent proteins where

9 Helix D is the first structural element to gain protection during refolding. Blue bars

1 represent proteins where Helix A is the first structural element to gain protection during
2 refolding. Grey bars represent proteins where the helix protection order could not be
3 unambiguously determined. The order of helix protection for each ancestor and
4 homolog is also colored on the phylogenetic tree, revealing a trend in the RNase H
5 folding trajectory along the evolutionary lineages. The phylogenetic tree shown in this
6 figure is adapted from Figure 2A of Hart KM et al. 2014, *PLoS Biology*. 12(11)
7 doi:10.1371/journal.pbio.1001994, published under the Creative Commons Attribution
8 4.0 International Public License (CC BY 4.0;
9 <https://creativecommons.org/licenses/by/4.0/>).³¹



1
2 **Figure 5. Engineered mutations to alter the folding pathway of ecRNH***
3 **A)** Crystal structure of *E. coli* RNase H (PDB: 2RN2) with mutations designed to alter
4 intrinsic helicity.⁵⁵ A55G, located in Helix A (blue), is colored in cyan. D108L, located in
5 Helix D (green), is colored in light green. **B)** Protection of peptides mapping to distinct
6 secondary structural elements of ecRNH* A55G at 13 msec after refolding. Bars
7 represent the mean and standard deviation of each data set. $p = 0.0917$ (n.s. = not
8 significant, Welch's unpaired T-test). **C)** Protection of peptides mapping to distinct
9 secondary structural elements of ecRNH* D108L at 13 msec after refolding. Bars
10 represent the mean and standard deviation of each data set. * $p = 0.0016$, ** $p = 0.0044$
11 (Welch's unpaired T-test)

Supplemental Materials

Tracing a protein's folding pathway over evolutionary time using ancestral sequence reconstruction and hydrogen exchange

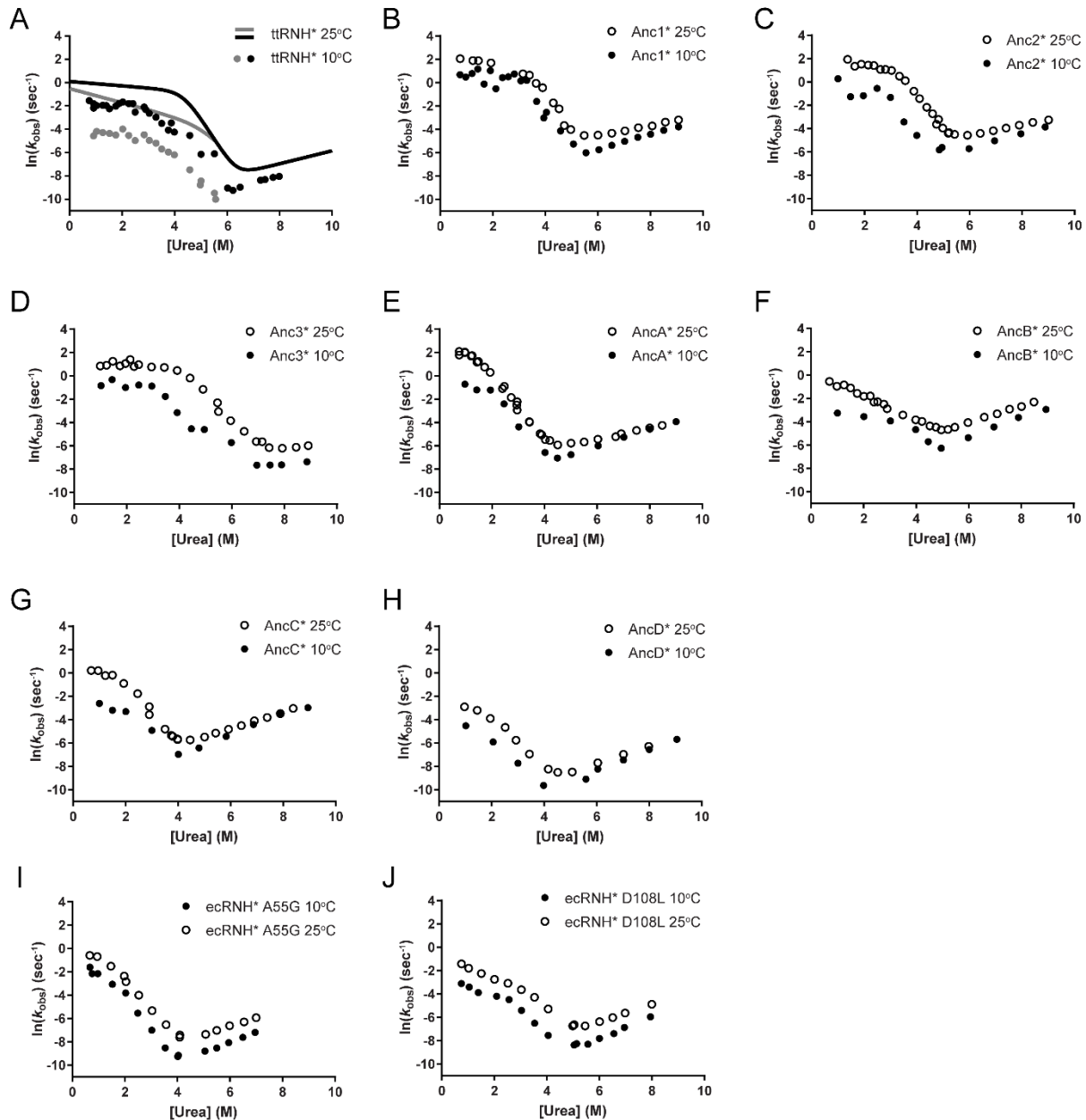


Figure S1. Chevron plot of RNase H variants studied at 10°C and 25°C

Chevron plots ($\ln(k_{obs})$ vs [urea]), determined from refolding and unfolding experiments in various [urea] at 10°C and 25°C for **A**) ttRNH*, **B**) Anc1*, **C**) Anc2*, **D**) Anc3*, **E**)

AncA*, **F)** AncB*, **G)** AncC*, **H)** AncD*, **I)** ecRNH* A55G, **J)** ecRNH* D108L. For **A)** Both the fast (black dots) and slow (grey dots) rates of folding for ttRNH* are shown at 10°C, and chevron fits for the two rates at 25°C are shown as lines and adapted from previous work.¹ Data at 25°C for **B)** – **H)** were adapted from a previously published study.²

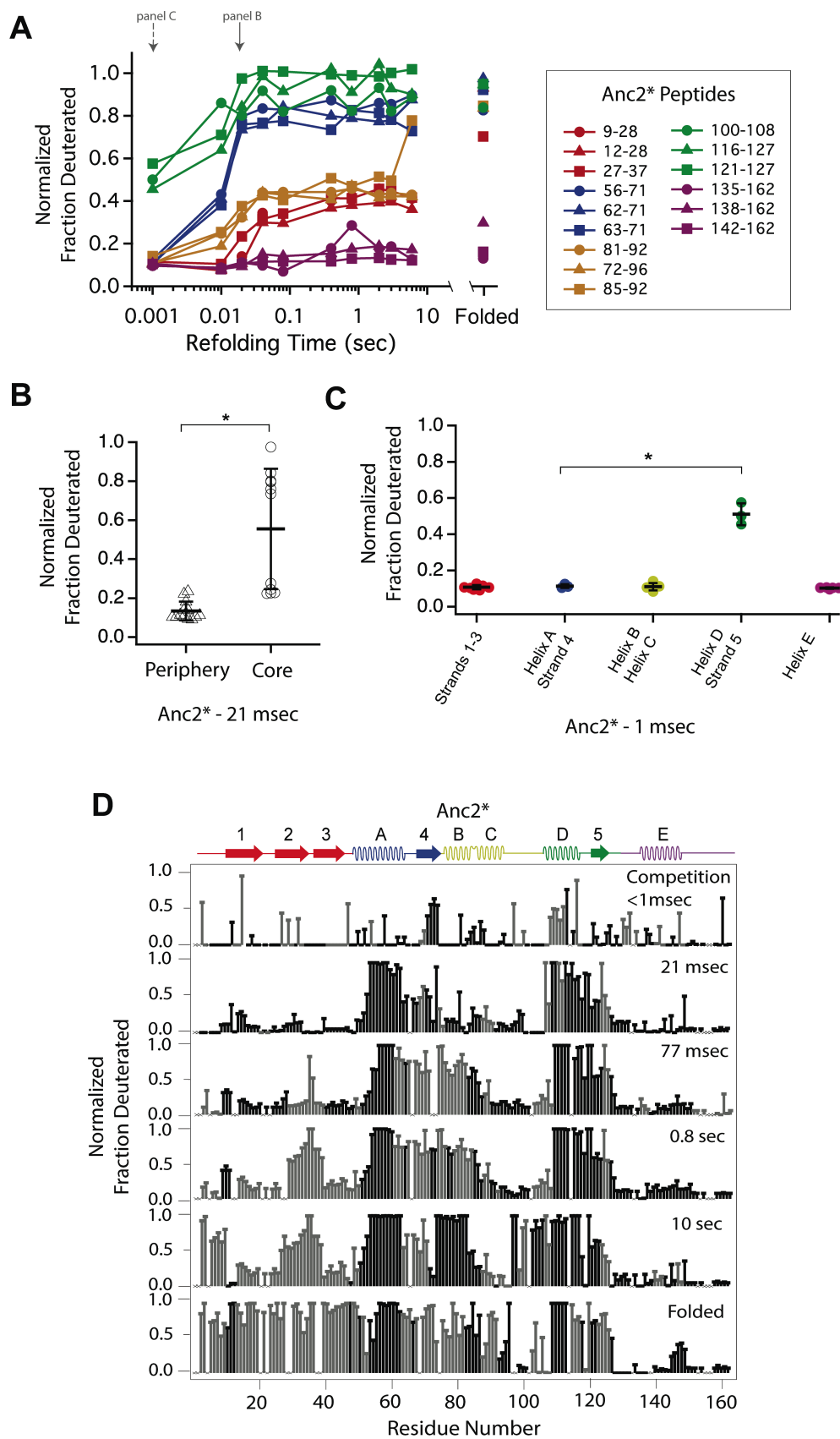


Figure S2. Determination of the folding pathway of Anc2* by HX-MS

A) Protection of representative peptides from Anc2* at various refolding times. Peptides are colored according to their corresponding structural element. The solid arrow indicates the refolding time point analyzed in panel B. The dotted arrow indicates the refolding time point analyzed in panel C. **B)** Protection of peptides mapping to the core region (I_{core}) or the periphery region of Anc2* at 21 msec after refolding. Bars represent the mean and standard deviation of each data set. * $p = 0.0011$ (Welch's unpaired T-test) **C)** Protection of peptides of Anc2* mapping to distinct secondary structural elements at 1 msec after refolding. Bars represent the mean and standard deviation of each data set. * $p = 0.0064$ (Welch's unpaired T-test). **D)** Residue-resolved folding pathway of Anc2* at representative refolding time points. Data points in black indicate residues that are site-resolved. Data points in grey indicate residues in regions with less peptide coverage and are thus not site-resolved with the neighboring residues. Residues where site-resolved protection could not be determined due to insufficient peptide coverage is denoted with a "x".

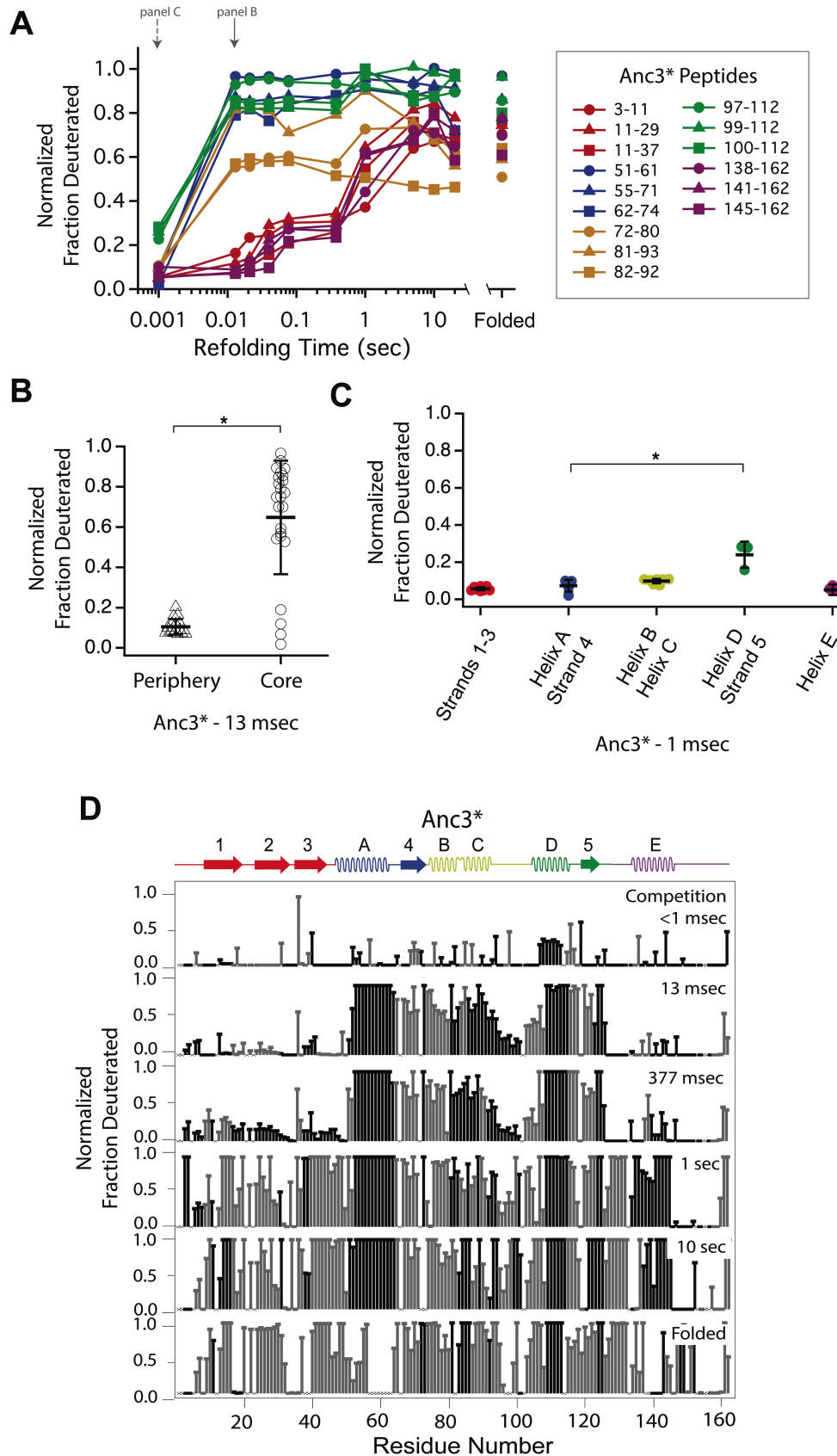


Figure S3. Determination of the folding pathway of Anc3* by HX-MS

A) Protection of representative peptides from Anc3* at various refolding times. Peptides are colored according to their corresponding structural element. The solid arrow indicates the refolding time point analyzed in panel B. The dotted arrow indicates the refolding time point analyzed in panel C. **B)** Protection of peptides mapping to the core region (I_{core}) or the periphery region of Anc3* at 13 msec after refolding. Bars represent the mean and standard deviation of each data set. * $p < 0.0001$ (Welch's unpaired T-test) **C)** Protection of peptides of Anc3* mapping to distinct secondary structural elements at 1 msec after refolding. Bars represent the mean and standard deviation of each data set. * $p = 0.0419$ (Welch's unpaired T-test). **D)** Residue-resolved folding pathway of Anc3* at representative refolding time points. Data points in black indicate residues that are site-resolved. Data points in grey indicate residues in regions with less peptide coverage and are thus not site-resolved with the neighboring residues. Residues where site-resolved protection could not be determined due to insufficient peptide coverage is denoted with a "x".

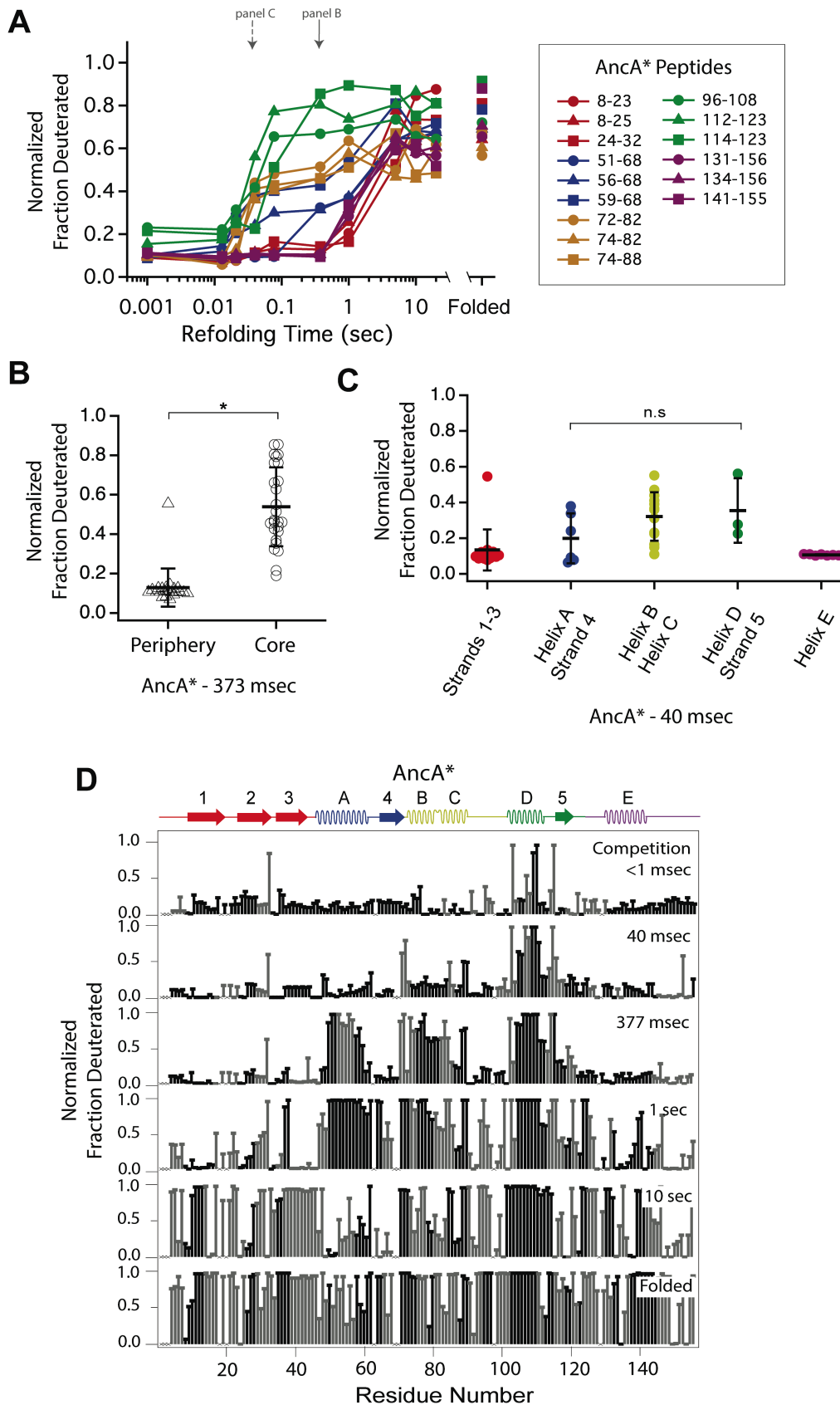


Figure S4. Determination of the folding pathway of AncA* by HX-MS

A) Protection of representative peptides from AncA* at various refolding times. Peptides are colored according to their corresponding structural element. The solid arrow indicates the refolding time point analyzed in panel B. The dotted arrow indicates the refolding time point analyzed in panel C. **B)** Protection of peptides mapping to the core region (I_{core}) or the periphery region of AncA* at 373 msec after refolding. Bars represent the mean and standard deviation of each data set. * $p < 0.0001$ (Welch's unpaired T-test) **C)** Protection of peptides of AncA* mapping to distinct secondary structural elements at 40 msec after refolding. Bars represent the mean and standard deviation of each data set. $p = 0.275$ (n.s. = not significant, Welch's unpaired T-test). **D)** Residue-resolved folding pathway of AncA* at representative refolding time points. Data points in black indicate residues that are site-resolved. Data points in grey indicate residues in regions with less peptide coverage and are thus not site-resolved with the neighboring residues. Residues where site-resolved protection could not be determined due to insufficient peptide coverage is denoted with a "x".

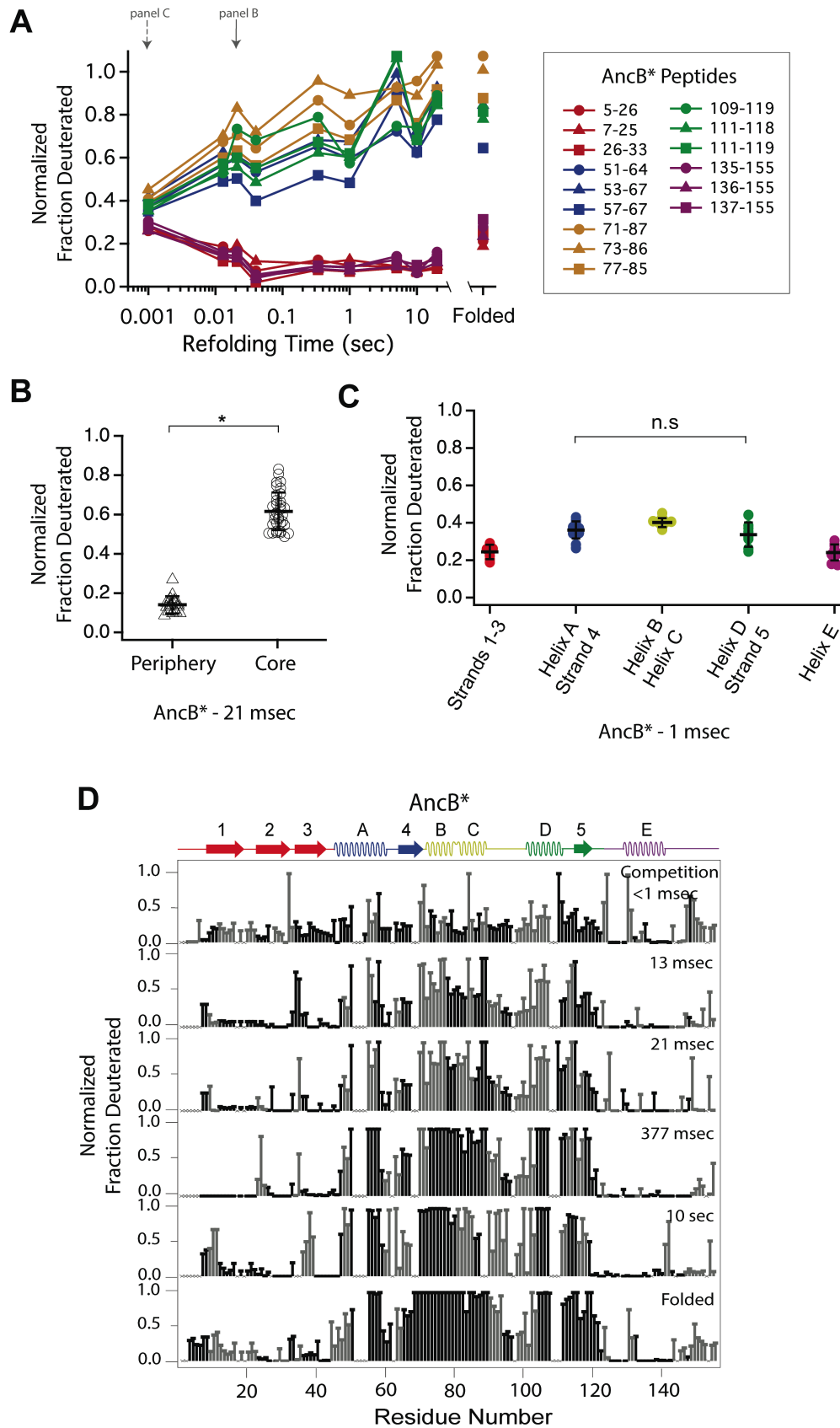


Figure S5. Determination of the folding pathway of AncB* by HX-MS

A) Protection of representative peptides from AncB* at various refolding times. Peptides are colored according to their corresponding structural element. The solid arrow indicates the refolding time point analyzed in panel B. The dotted arrow indicates the refolding time point analyzed in panel C. **B)** Protection of peptides mapping to the core region (I_{core}) or the periphery region of AncB* at 21 msec after refolding. Bars represent the mean and standard deviation of each data set. * $p < 0.0001$ (Welch's unpaired T-test) **C)** Protection of peptides of AncB* mapping to distinct secondary structural elements at 1 msec after refolding. Bars represent the mean and standard deviation of each data set. $p = 0.353$ (n.s. = not significant, Welch's unpaired T-test). **D)** Residue-resolved folding pathway of AncB* at representative refolding time points. Data points in black indicate residues that are site-resolved. Data points in grey indicate residues in regions with less peptide coverage and are thus not site-resolved with the neighboring residues. Residues where site-resolved protection could not be determined due to insufficient peptide coverage is denoted with a "x".

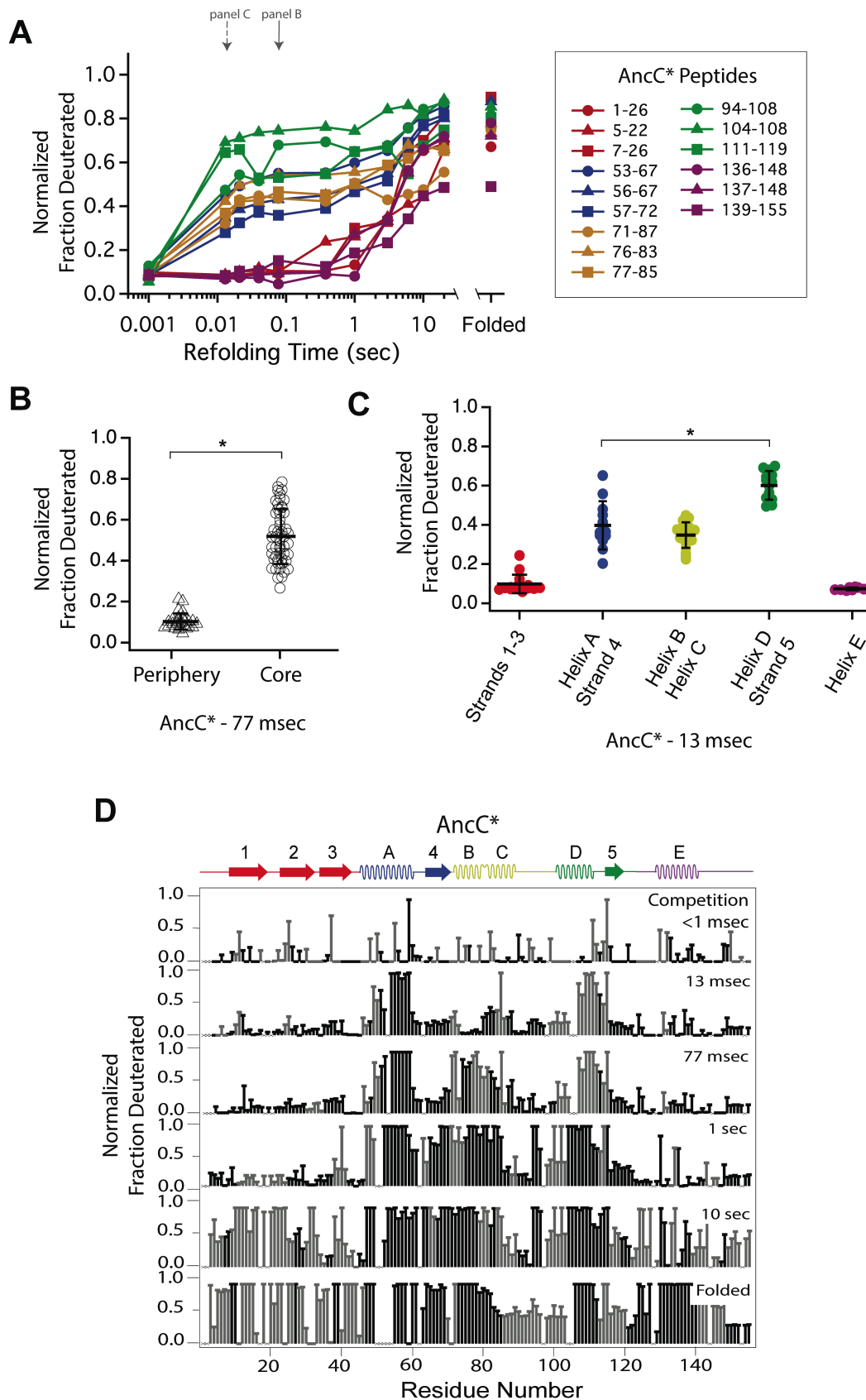


Figure S6. Determination of the folding pathway of AncC* by HX-MS

A) Protection of representative peptides from AncC* at various refolding times. Peptides are colored according to their corresponding structural element. The solid arrow indicates the refolding time point analyzed in panel B. The dotted arrow indicates the refolding time point analyzed in panel C. **B)** Protection of peptides mapping to the core region (I_{core}) or the periphery region of AncC* at 77 msec after refolding. Bars represent the mean and standard deviation of each data set. * $p < 0.0001$ (Welch's unpaired T-test) **C)** Protection of peptides of AncC* mapping to distinct secondary structural elements at 13 msec after refolding. Bars represent the mean and standard deviation of each data set. * $p < 0.0001$ (Welch's unpaired T-test). **D)** Residue-resolved folding pathway of AncC* at representative refolding time points. Data points in black indicate residues that are site-resolved. Data points in grey indicate residues in regions with less peptide coverage and are thus not site-resolved with the neighboring residues. Residues where site-resolved protection could not be determined due to insufficient peptide coverage is denoted with a "x".

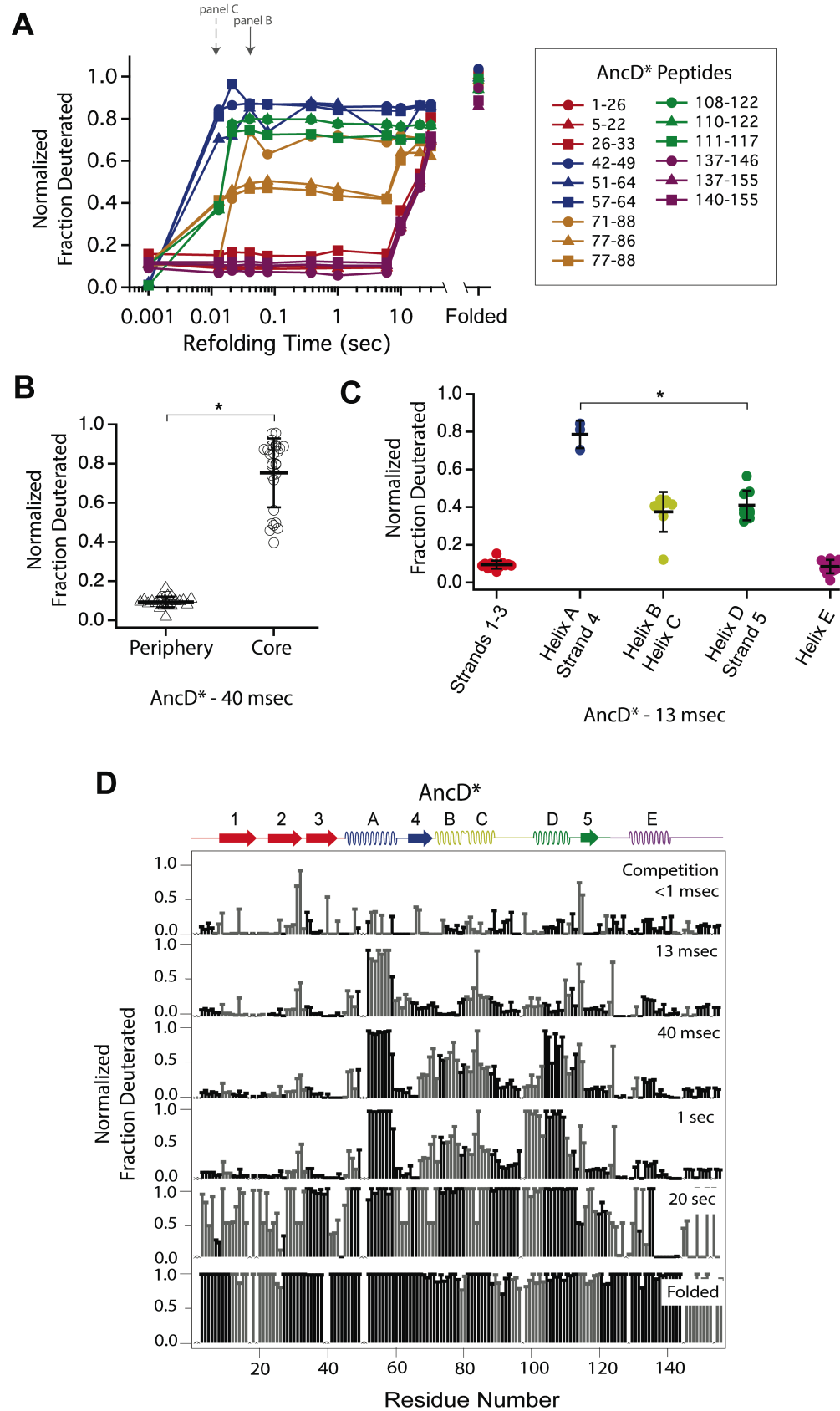


Figure S7. Determination of the folding pathway of AncD* by HX-MS

A) Protection of representative peptides from AncD* at various refolding times. Peptides are colored according to their corresponding structural element. The solid arrow indicates the refolding time point analyzed in panel B. The dotted arrow indicates the refolding time point analyzed in panel C. **B)** Protection of peptides mapping to the core region (I_{core}) or the periphery region of AncD* at 40 msec after refolding. Bars represent the mean and standard deviation of each data set. * $p < 0.0001$ (Welch's unpaired T-test) **C)** Protection of peptides of AncD* mapping to distinct secondary structural elements at 13 msec after refolding. Bars represent the mean and standard deviation of each data set. * $p = 0.021$ (Welch's unpaired T-test). **D)** Residue-resolved folding pathway of AncD* at representative refolding time points. Data points in black indicate residues that are site-resolved. Data points in grey indicate residues in regions with less peptide coverage and are thus not site-resolved with the neighboring residues. Residues where site-resolved protection could not be determined due to insufficient peptide coverage is denoted with a "x".

Table S1. Comparison of intrinsic helicity and AABUF across RNase H variants

	ttRNH*		Anc3*		Anc2*		Anc1*	
	AABUF (Å ²) [†]	Helicity (%) [‡]	AABUF (Å ²)	Helicity (%)	AABUF (Å ²)	Helicity (%)	AABUF (Å ²)	Helicity (%)
Helix A	122.35	3.61	122.35	3.56	124.57	1.74	124.57	1.82
Helix D	135.97	8.55	130.04	5.11	136.91	17.57	136.91	20.28
Ratio	0.90	0.42	0.94	0.70	0.91	0.10	0.91	0.09
Log2(Ratio)	-0.15	-1.24	-0.09	-0.52	-0.14	-3.34	-0.14	-3.48

	AncA*		AncB*		AncC*		AncD*	
	AABUF (Å ²)	Helicity (%)	AABUF (Å ²)	Helicity (%)	AABUF (Å ²)	Helicity (%)	AABUF (Å ²)	Helicity (%)
Helix A	124.57	1.92	126.35	3.22	128.56	5.34	128.62	10.04
Helix D	130.36	2.59	131.49	4.63	136.17	4.05	129.95	2.48
Ratio	0.96	0.74	0.96	0.69	0.94	1.32	0.99	4.05
Log2(Ratio)	-0.07	-0.43	-0.06	-0.53	-0.08	0.40	-0.01	2.02

	ecRNH*		ecRNH* A55G		ecRNH* D108L	
	AABUF (Å ²)	Helicity (%)	AABUF (Å ²)	Helicity (%)	AABUF (Å ²)	Helicity (%)
Helix A	128.62	9.66	127.23	3.01	128.62	9.66
Helix D	129.95	2.47	129.95	2.47	134.37	20.28
Ratio	0.99	3.92	0.98	1.22	0.96	0.48
Log2(Ratio)	-0.01	1.97	-0.03	0.29	-0.06	-1.07

[†] AABUF values are the average across each helix as predicted using values from Rose, et al. (1985).

[‡] Helicity values are the average across each helix as predicted using values from Muñoz and Serrano (1994).

References for Supplemental Materials

- Hollien, J. & Marqusee, S. Comparison of the folding processes of *T. thermophilus* and *E. coli* ribonucleases H. *J. Mol. Biol.* **316**, 327–340 (2002).
- Lim, X.-X. *et al.* Epitope and Paratope Mapping Reveals Temperature-Dependent Alterations in the Dengue-Antibody Interface. *Structure* **25**, 1391–1402.e3 (2017).
- Muñoz, V. & Serrano, L. Elucidating the folding problem of helical peptides using empirical parameters. *Nat. Struct. Biol.* **1**, 399–409 (1994).
- Rose, G. D., Geselowitz, A. R., Lesser, G. J., Lee, R. H. & Zehfus, M. H. Hydrophobicity of amino acid residues in globular proteins. *Science* **229**, 834–838 (1985).
- Nishimura, C., Prytulla, S., Jane Dyson, H. & Wright, P. E. Conservation of folding pathways in evolutionarily distant globin sequences. *Nat. Struct. Biol.* **7**, 679–686 (2000).